
Variational Inference of overparameterized Bayesian Neural Networks: a theoretical and empirical study

Tom Huix

CMAP, Ecole Polytechnique
IP Paris

tom.huix@polytechnique.edu

Szymon Majewski

CMAP, Ecole Polytechnique
IP Paris

sjm.majewski@gmail.com

Alain Durmus

ENS Paris-Saclay
Université Paris-Saclay

alain.durmus@ens-paris-saclay.fr

Eric Moulines

CMAP, Ecole Polytechnique
IP Paris

eric.moulines@polytechnique.edu

Anna Korba

ENSAE, CREST
IP Paris

anna.korba@ensae.fr

Abstract

This paper studies the Variational Inference (VI) used for training Bayesian Neural Networks (BNN) in the overparameterized regime, *i.e.*, when the number of neurons tends to infinity. More specifically, we consider overparameterized two-layer BNN and point out a critical issue in the mean-field VI training. This problem arises from the decomposition of the lower bound on the evidence (ELBO) into two terms: one corresponding to the likelihood function of the model and the second to the Kullback-Leibler (KL) divergence between the prior distribution and the variational posterior. In particular, we show both theoretically and empirically that there is a trade-off between these two terms in the overparameterized regime only when the KL is appropriately re-scaled with respect to the ratio between the number of observations and neurons. We also illustrate our theoretical results with numerical experiments that highlight the critical choice of this ratio.

1 Introduction

Bayesian neural networks (BNN) have gained popularity in the field of machine learning because they promise to combine the powerful approximation/discrimination properties of (deep) neural networks (NN) with the decision-theoretic approach of Bayesian inference. Among the advantages of BNN is their ability to provide uncertainty quantification, which is a must in many fields - e.g., autonomous driving [Michelmor et al. \(2020\)](#); [McAllister et al. \(2017\)](#), computer vision [Kendall and Gal \(2017\)](#), medical diagnosis [Filos et al. \(2019\)](#). Second, the inclusion of prior information in some cases leads to better generalization error and calibration in classification tasks; see [Jospin et al. \(2020\)](#); [Izmailov et al. \(2021\)](#) and references therein.

NN can be used to build complex probabilistic models for regression and classification tasks. Given \bar{w} corresponding to the weights and bias of an NN, the network output can be used to define a (conditional) likelihood $L(\{(x_i, y_i)\}_{i=1}^p | \bar{w})$ of some observed labels $\{y_i\}_{i=1}^p$, $y_i \in \mathcal{Y}$ associated with feature vectors $\{x_i\}_{i=1}^p$, $x_i \in \mathcal{X}$. Specifying a prior distribution for \bar{w} and applying Bayes' rule

yields the posterior distribution of weights. In the Bayesian approach, the goal is to find the predictive distribution from new feature vectors defined as an integral with respect to the posterior. One possible approach is to use Markov-Chain Monte Carlo methods - such as Hamiltonian Monte Carlo - for inference in Bayesian neural networks; Neal et al. (2011); Hoffman et al. (2014); Betancourt (2017). However, the challenge of scaling HMC for applications involving high-dimensional parameter space and large datasets limits its broad application; Cobb and Jalaian (2021). Computationally cheaper MCMC methods have been proposed, see Welling and Teh (2011); Chen et al. (2014); Brosse et al. (2018); but these methods yield biased estimates of posterior expectation, see Izmailov et al. (2021). A much simpler alternative from a computational standpoint is to use Variational Inference (VI) Blundell et al. (2015); Gal and Ghahramani (2016); Louizos and Welling (2017); Khan et al. (2018), which approximates the posterior with a parametric distribution. Nevertheless, little is known about the validity or limitations of the latter approach, including the choice of prior and variational family and their interplay.

A number of recent papers have investigated the limiting behavior of gradient descent type algorithms for one or two hidden layers in the overparameterized regime, Chizat and Bach (2018); Rotkoff et al. (2019); Mei et al. (2018); Tzen and Raginsky (2019); De Bortoli et al. (2020), *i.e.*, the number of hidden neurons goes to infinity. More specifically, it was found that the gradient descent applied to risk minimization can be viewed as a temporal and spatial discretization of the Wasserstein gradient flow of a limiting function, which can be represented in the space of probability distributions over the parameters by

$$R_\mu(\mu) = \int \ell(y, \int s(\bar{w}, x) d\mu(\bar{w})) d\pi(x, y) + N(\mu), \quad (1)$$

where π is the data distribution over $X \times Y$, $s(\bar{w}, x)$ is the output prediction of the NN with parameter weights \bar{w} and N plays the role of a penalty function. Roughly speaking, identifying this function consists in noting that the risk R_w over the weights \bar{w} of a NN coincides with R_μ on the set of empirical measures, *i.e.* for any $\bar{w} = (w_1, \dots, w_N)$ - where N is the number of neurons-, $R_w(\bar{w}) = R_\mu(\mu_N)$ with $\mu_N = N^{-1} \sum_{i=1}^N \delta_{w_i}$. This result emphasizes that in the overparameterized regime, the parameter weights of a NN act as particle discretization of probability measures and the final prediction of a NN has a form of continuous mixture.

We are interested here in performing the same type of analysis but for Variational Inference (VI) of two layer Bayesian Neural Networks (BNN). In this setting, the parameter weights for making predictions in practice are no longer fixed, but are sampled from a variational posterior, and the final result is the empirical average of the prediction of each sample. This variational posterior is obtained by maximizing an objective function, the Evidence Lower Bound (ELBO) over a parameter space Ξ^N . It was empirically found that the maximization of the "vanilla" ELBO function - based on the "vanilla" posterior distribution of a BNN-, can yield very poor inferences. To address this problem, a modification of this objective function was proposed, resulting from a decomposition into two terms of this function: one corresponding to the Kullback-Leibler (KL) divergence between the variational density and the prior and the other to a marginal likelihood term. Based on this decomposition, the modified version of ELBO, called partially tempered ELBO, consists in multiplying the KL term by a temperature parameter.

Although this change has been justified intuitively or by purely statistical considerations, to our knowledge no formal results have been derived. Our first contribution is to show that this procedure is indeed mandatory in the overparameterized regime. More precisely, we show that if the temperature is not scaled appropriately with respect to the number of neurons and data points, one of the two terms becomes dominant and therefore either the resulting posterior is too close to the prior - underfitting- or overfitting occurs. Our second contribution is to identify, similarly to risk minimization, a limiting function for the partially tempered version of ELBO when the number of neurons and data points approaches infinity and the temperature parameter is appropriately chosen. Our conclusions are twofold. First, we highlight the importance of the choice of prior and variational family for the resulting variational posterior distribution. Second, we show that performing VI for BNN in the overparameterized regime is equivalent to risk over an extended space of probability measures. In summary, then, the use of VI for BNN enriches traditional NN models by producing predictions from a hierarchical mixture distribution. Ultimately, this shows that using VI to train overparameterized BNN amounts to empirical risk minimization and therefore should be interpreted with caution for performing Bayesian uncertainty quantification, as our contributions imply that

the resulting posterior does not concentrate as the number of observations grows and is therefore not related to the usual Bayesian posterior distribution of the model.

This paper is organized as follows. Section 2 introduces the background of VI on BNN. Section 3 characterizes the inadequacy of these models in the limiting case of the mean field, when the data or prior variance do not scale, and identifies the well-posed regime. In Section 4, some numerical experiments are presented to illustrate our claims.

Notations. We assume that \mathbb{R}^d is equipped with the Euclidean topology. For any set $E \subset \mathbb{R}^d$, we denote by $\mathcal{P}(E)$ the set of probability measures on E equipped with the trace topology and the trace σ -field denoted by \mathcal{E} . We define the weak topology on $\mathcal{P}(E)$ as the initial topology associated with $\nu \in \mathcal{P}(E) \mapsto \int f d\nu$ for bounded and continuous map $f : E \rightarrow \mathbb{R}$. For any $\nu, \mu \in \mathcal{P}(E)$ we denote by $\nu \otimes \mu$ the product measure and define by induction $\nu^{\otimes N} = \nu^{\otimes N-1} \otimes \nu$. For $\sigma \in \mathbb{R}^d$, the diagonal matrix in $\mathbb{R}^{d \times d}$ with diagonal $\sigma^2 = [\sigma_1^2, \dots, \sigma_d^2]$ will be denoted $\text{diag}(\sigma^2)$. For any measurable map $\mathcal{T} : \mathbb{R}^d \times \mathbb{R}^d$ and probability measure $\nu \in \mathcal{P}(\mathbb{R}^d)$, we denote by $\mathcal{T}_\# \nu$ the pushforward measure of ν by \mathcal{T} . It is characterized by the transfer lemma, i.e. $\int F(y) d\mathcal{T}_\# \nu(y) = \int F(\mathcal{T}(z)) d\nu(z)$ for any measurable and bounded function F . For $\mu, \pi \in \mathcal{P}(E)$, the Kullback-Leibler divergence between a distribution μ and π is defined by $\text{KL}(\mu|\pi) = \int \log(d\mu/d\pi) d\mu$ where $d\mu/d\pi$ is the Radon-Nikodym derivative if μ is absolutely continuous with respect to π , and $\text{KL}(\mu|\pi) = +\infty$ otherwise.

2 Variational inference for BNN objective

Consider a supervised setting where we have access to i.i.d. samples $\{(x_i, y_i)\}_{i=1}^p$, from a distribution π on $X \times Y \subset \mathbb{R}^{d_X} \times \mathbb{R}^{d_Y}$, and aim at predicting y given a new observation x . In this paper, we focus on a fully connected NN with one hidden layer and N neurons, and activation function $h : \mathbb{R}^{d_X} \times X \rightarrow \mathbb{R}$. A common example of such a function is

$$h(b_j, x) = \sigma(\langle b, x \rangle), \quad (2)$$

for $b \in \mathbb{R}^{d_X}$ and $x \in X$, where $\sigma : \mathbb{R} \rightarrow \mathbb{R}$ is the Rectified Linear Unit $\sigma(t) = \max(0, t)$ or sigmoid function $\sigma(t) = e^t / (1 + e^t)$, for $t \in \mathbb{R}$. In addition, for $j \in \{1, \dots, N\}$, denote by $b_j \in \mathbb{R}^{d_X}$ and $a_j \in \mathbb{R}^{d_Y}$ the j -th weights of the hidden and output layers respectively, and set $w_j = (b_j, a_j) \in \mathbb{R}^d$, $d = d_X + d_Y$, $\bar{w} = (w_j)_{j=1}^N$ all the weights of the NN under consideration. With this notation, for each input $x \in X$, the output prediction $f_{\bar{w}} : X \rightarrow \mathbb{R}^{d_Y}$ of the neural network can be written as:

$$f_{\bar{w}}(x) = N^{-1} \sum_{j=1}^N s(w_j, x), \text{ with } s(w_j, x) = a_j h(b_j, x). \quad (3)$$

Given a loss function $\ell : Y \times Y \rightarrow \mathbb{R}_+$, we use the prediction function $f_{\bar{w}}$ to define the conditional likelihood

$$L(y|x, \bar{w}) \propto \exp(-\ell(f_{\bar{w}}(x), y)), \quad (4)$$

with respect to the Lebesgue measure on $\mathbb{R}^{d \times N}$ denoted by $\text{Leb}_{d \times N}$. Then, choosing a prior pdf P_0 on \bar{w} , the posterior pdf P of the weights is proportional to $\bar{w} \mapsto P_0(\bar{w}) \prod_{i=1}^p L(y_i|x_i, \bar{w})$. We perform Bayesian inference using VI (Khan and Rue, 2021; Blei et al., 2017; Blundell et al., 2015; Graves, 2011; Khan et al., 2018). The general procedure is to consider a variational family of pdfs $\mathcal{F}_\Theta = \{q_\theta : \theta \in \Theta\}$, for $\Theta \subset \mathbb{R}^{d_\theta}$ and the Evidence Lower Bound (ELBO) defined for any $\theta \in \Theta$ by:

$$\text{ELBO}^N(\theta) = -\text{KL}(q_\theta | P_0) + \sum_{i=1}^p \int_{\mathbb{R}^{N \times d}} \log L(y_i|x_i, \bar{w}) q_\theta(\bar{w}) d\text{Leb}_{d \times N}(\bar{w}). \quad (5)$$

It is known that maximizing ELBO^N is equivalent to minimizing $\theta \mapsto \text{KL}(q_\theta | P)$. For this reason, VI consists in approximating the posterior distribution by q_{θ^*} with $\theta^* \in \arg\max \text{ELBO}^N$. The first term in (5) acts as a penalty term to control the deviation of q_{θ^*} from the prior P_0 , while the second term plays the role of empirical risk and promotes adaptation of the data. In practice, however, it has been shown that the choice of the prior and the variational approximation ELBO^N is crucial for good performance. It was proposed by Zhang et al. (2018); Khan et al. (2018); Osawa

et al. (2019); Ashukha et al. (2020) to weaken the regularization term KL and consider a partially tempered version of ELBO^N , which for a cooling parameter $\eta_N > 0$ is given by

$$\text{ELBO}_\eta^N(\theta) = -\eta_N \text{KL}(q_\theta | P_0) + \sum_{i=1}^p \int_{\mathbb{R}^{N \times d}} \log L(y_i | x_i, \bar{w}) q_\theta(\bar{w}) d\text{Leb}_{d \times N}(\bar{w}). \quad (6)$$

It has been shown in Wenzel et al. (2020); Wilson and Izmailov (2020) that ELBO_η^N is the same as ELBO^N but considering instead of the common posterior P , a partially tempered posterior $P_{T_N} \propto L^{1/T_N} P_0$, where the likelihood function is tempered for some temperature $T_N \geq 0$. The parameter η_N (or equivalently the temperature T_N) controls the tradeoff of the likelihood term with respect to the prior. Setting $\eta_N < 1$ corresponds to a *cold posterior*, where the likelihood term is strengthened so that the posterior is concentrated in regions of high likelihood. The case $\eta_N = 1$ corresponds to "plain" Bayesian inference, while $\eta_N < 1$ corresponds to *warm posterior* where the prior has a stronger influence on the posterior.

In a series of paper, Grünwald (2012); Grünwald and Van Ommen (2017); Bhattacharya et al. (2019); Heide et al. (2020); Grunwald et al. (2021) have shown - significantly extending earlier results of Barron and Cover (1991); Zhang (2006) - that partially tempered posteriors may have better statistical properties under model misspecification than the "plain" posterior as the number of data points goes to infinity (expressed in terms posterior contraction around the best approximation of the truth). These results have been derived for Generalized Linear Models and it is not clear how these results extend to BNN. Wilson and Izmailov (2020) more informally argues that tempering is not inconsistent with Bayesian principles and that it may be particularly relevant in a parametric setting (where the model is defined by parameters), as opposed to Bayesian Nonparametric approaches - e.g., Gaussian processes. Namely, while in nonparametric approaches the model capacity is automatically scaled with the available data, this is not the case in parametric approaches, where the model capacity (which is determined by the number of neurons and the neural network architecture) is chosen by the user. Model misspecification is the rule in such case, as we show in Section 3 for neural networks with a hidden layer. However, to the best of our knowledge, the temperature scaling with respect to the number of data points and network parameters has not been investigated theoretically, in particular in the context of BNN.

Other studies, e.g., Farquhar et al. (2019), noted that a potential cause of the predominance of the KL term in (5) stems from the choice of the prior. Indeed, it has been noticed that the role of P_0 is important since it lead to very different inferences, see Fortuin (2021). In particular, using priors on \bar{w} which factorize over the weights, *i.e.*, of the form

$$P_0(\bar{w}) = \prod_{j=1}^N P_0^1(w_j), \quad (7)$$

do not yield optimal performance and as a result Tran et al. (2020); Fortuin et al. (2021); Ober and Aitchison (2021); Sun et al. (2019) have proposed the design of new priors which introduce correlation amongst the weights and/or heavier tails than Gaussian ones.

In the present work, we take a novel approach to justify the use of ELBO_η^N based on the so-called overparameterized regime and study the impact of the choice of the cooling parameter η_N . We assume that the prior factorizes over the neurons, *i.e.*, the prior takes the form (7) and for each $\theta = (\theta_1, \dots, \theta_N) \in \Xi^N$, $q_\theta(\bar{w}) = \prod_{i=1}^N q_{\theta_j}^1(w_j)$, where P_0^1 and $\{q_{\theta_j}^1\}_{j=1}^N$ are distributions over $\Xi \subset \mathbb{R}^d$. In this case, $\Theta = \Xi^N$ and the prior distribution for each neuron P_0^1 is the same. Further, we assume that for any $\theta \in \Xi$, the variational distribution corresponding to q_θ^1 is the pushforward of a reference probability measure with density γ by \mathcal{T}_θ , where $\{\mathcal{T}_\theta : \theta \in \Xi\}$ is a family of C^1 -diffeomorphisms on \mathbb{R}^d , *i.e.*, $q_\theta^1(w) = \gamma(\mathcal{T}_\theta^{-1}(w)) J_{\mathcal{T}_\theta^{-1}}(w)$, denoting by $J_{\mathcal{T}_\theta^{-1}}$ the Jacobian determinant of \mathcal{T}_θ^{-1} . A common choice for \mathcal{T}_θ is, setting $\theta = (\mu, \sigma) \in \mathbb{R}^d \times (\mathbb{R}_+^*)^d$,

$$\mathcal{T}_\theta : z \mapsto \mu + \sigma \odot z, \quad (8)$$

where \odot is the component wise product but of course much more sophisticated choices are possible. Then, by (3)-(4) and a change of variable, the ELBO can be expressed as

$$\text{ELBO}_\eta^N(\theta) = - \sum_{i=1}^p G_\Theta^N(\theta; (x_i, y_i)) - \eta_N \sum_{j=1}^N \text{KL}(q_{\theta_j}^1 | P_0^1) \quad (9)$$

with denoting the output of a neuron parametrized by $\theta \in \mathbb{R}^d$ for an input x_i by

$$\phi(\theta, z, x_i) = s(\mathcal{T}_\theta(z), x_i), \quad (10)$$

and $\mathbf{z} = (z_1, \dots, z_N) \in \mathbb{R}^{d \times N}$,

$$G_\Theta^N(\boldsymbol{\theta}; (x, y)) = \int \ell \left(y, \sum_{j=1}^N \frac{\phi(\theta_j, z_j, x)}{N} \right) \gamma^{\otimes N}(\mathrm{d}\mathbf{z}). \quad (11)$$

Although the VI framework we are considering may seem overly simplistic in light of the above, it is the one most commonly used in practice, and therefore it is still very important to obtain useful guidelines for implementation in order to optimize its performance. Moreover, it is a first step before considering other VI methods with more complex priors and/or variational families. The expression of ELBO_η^N shows that the parameter η_N must be chosen to balance the two terms in (6) to obtain a well-posed VI functional as $N, p \rightarrow +\infty$ and a variational posterior $q_{\boldsymbol{\theta}^*}$ different from the prior. Without this parameter, optimizing the ELBO^N (5) leads to the collapse of the variational posterior to the prior, as shown in the following proposition.

Proposition 1. Assume that \mathcal{F}_Θ is a family of Gaussians with diagonal covariance matrices, that $P_0 \in \mathcal{F}_\Theta$ and that \mathbf{X} is compact. Let $\boldsymbol{\theta}^{*,N} = \operatorname{argmax}_{\boldsymbol{\theta} \in \Theta} \text{ELBO}_\eta^N(\boldsymbol{\theta})$. Assume also that l is the square loss or cross-entropy, and that σ is Lipschitz. Then, $\text{KL}(q_{\boldsymbol{\theta}^{*,N}}, P_0) \rightarrow 0$ as $N \rightarrow \infty$.

This result and its proof, that can be found in Appendix B, are inspired from Coker et al. (2021, Theorem 1,2) that show that the moments of the predictive posterior collapse to the ones of the prior and that the KL converges to 0 as $N \rightarrow \infty$, when l is the square loss and σ is odd. Proposition 1 states an analog result, but which holds for additional losses (i.e., also cross-entropy) and more general activation functions (e.g., non odd ones as ReLU). This is partly due to our different scaling of the output of the neural network, in $O(1/N)$ (see (3)) that differs from theirs (in $O(1/\sqrt{N})$). The result of Proposition 1 highlights that optimizing ELBO_η^N becomes ill-posed as $N \rightarrow \infty$. This suggests that the optimal variational posterior tends to ignore the data fitting term in (9), and that η_N must be chosen to rebalance ELBO_η^N . In the next section, we provide a theoretical framework supporting this informal discussion and then present our main results regarding the choice of η_N .

3 Identifying well-posed regimes for the ELBO with product priors

We follow the approach outlined in Chizat and Bach (2018); Rotskoff et al. (2019); Mei et al. (2018) for ERM. We first generalize the definition of ELBO_η^N defined in (9) over Ξ^N to probability measures ν on Ξ . Indeed, the following result states that ELBO_η^N can be expressed as a functional of the empirical measure over the weights ν_N^θ defined for each $\boldsymbol{\theta} = (\theta_1, \dots, \theta_N) \in \Xi^N$ by

$$\nu_N^\theta = N^{-1} \sum_{i=1}^N \delta_{\theta_i}, \quad (12)$$

where δ_θ is the Dirac mass at $\theta \in \Xi$. Define $\mathcal{P}_N(\Xi)$ the subset of $\mathcal{P}(\Xi)$ which can be written as (12) for some $\boldsymbol{\theta} \in \Xi^N$.

Proposition 2. For any $N \in \mathbb{N}^*$, there exists a function F_η^N defined over $\mathcal{P}_N(\Xi)$ valued in $\mathbb{R} \cup \{+\infty\}$ such that $\text{ELBO}_\eta^N(\boldsymbol{\theta}) = F_\eta^N(\nu_N^\theta)$ for any $\boldsymbol{\theta} \in \Xi^N$.

Proof. Denote by \mathcal{S}_N the set of permutations $\tau : \{1, \dots, N\} \rightarrow \{1, \dots, N\}$ and for any $\boldsymbol{\theta} = (\theta_1, \dots, \theta_N) \in \Theta$, $\tau \in \mathcal{S}_N$, $\boldsymbol{\theta}^\tau = (\theta_{\tau(1)}, \dots, \theta_{\tau(N)})$. Note that for any $\tau \in \mathcal{S}_N$, $\text{ELBO}_\eta^N(\boldsymbol{\theta}) = \text{ELBO}_\eta^N(\boldsymbol{\theta}^\tau)$. The proof is then completed upon using that $\boldsymbol{\theta} \mapsto \nu_N^\theta$ is a bijection from Ξ^N / \sim to $\mathcal{P}_N(\Xi)$, where \sim is the equivalence relation defined by $\boldsymbol{\theta} \sim \boldsymbol{\theta}'$ if $\exists \tau \in \mathcal{S}_N$ s.t. $\boldsymbol{\theta}' = \boldsymbol{\theta}^\tau$. \square

Proposition 2 is a first step toward our results. However, its main caveat is that F_η^N cannot be non-trivially extended to a functional defined for a general probability measure on Ξ . However,

in our next result, we show that, when restricted to empirical probabilities, it is a perturbation, as $N \rightarrow +\infty$, of the functional \tilde{F}_η^N defined over all $\mathcal{P}(\Xi)$ by

$$\tilde{F}_\eta^N(\nu) = - \sum_{i=1}^p \tilde{G}(\nu; (x_i, y_i)) - \eta_N N \int \text{KL}(q_\theta^1 | P_0^1) d\nu(\theta) , \quad (13)$$

where

$$\tilde{G}(\nu; (x, y)) = \ell \left(y, \iint \phi(\theta, z, x) d\nu(\theta) d\gamma(z) \right) , \quad (14)$$

and ϕ is given by (10). We now define for any $\theta \in \Xi$ and $x \in \mathbf{X}$, $\tilde{\phi}(\theta, x) = \int \phi(\theta, z, x) d\gamma(z)$. Consider the following assumption:

A1. (i) There exists $L_\ell > 0$ such that for any $y \in \mathbf{Y}$, the function $\tilde{y} \mapsto \ell(y, \tilde{y})$ is L_ℓ -smooth: for any $\tilde{y}_1, \tilde{y}_2 \in \mathbf{Y}$,

$$\|\nabla_{\tilde{y}} \ell(y, \tilde{y}_1) - \nabla_{\tilde{y}} \ell(y, \tilde{y}_2)\| \leq L_\ell \|\tilde{y}_1 - \tilde{y}_2\| .$$

(ii) There exists $C_\phi \geq 0$, such that for any $\theta \in \Xi$ and $x \in \mathbf{X}$,

$$\int \left\| \phi(\theta, z, x) - \tilde{\phi}(\theta, x) \right\|^2 d\gamma(z) \leq C_\phi .$$

Note that A1-(i) is satisfied for the quadratic or logistic loss if \mathbf{Y} is bounded. We give practical conditions on the activation function σ , the prior P_0^1 and the set Ξ to ensure that A1-(ii) holds in the case where \mathcal{T}_θ is supposed to be of the form (8) for any $\theta \in \Xi$, later in this section after stating our general results.

Theorem 3. Assume A1. Then, there exists $C \geq 0$ such that for any $N, p \in \mathbb{N}^*$, $\{(x_i, y_i)\}_{i=1}^p \in (\mathbf{X} \times \mathbf{Y})^p$, $\theta \in \Xi^N$ and $\eta_N > 0$,

$$\left| \text{ELBO}_\eta^N(\theta) - \tilde{F}_\eta^N(\nu_N^\theta) \right| \leq Cp/N ,$$

where ν_N^θ is defined in (12).

Proof. Using that for any $y \in \mathbf{Y}$, the function $\tilde{y} \mapsto \ell(y, \tilde{y})$ is L_ℓ -smooth, we get by (Nesterov, 2004, Lemma 1.2.3), Proposition 2 and the definitions (9)-(11)-(13)-(14),

$$\begin{aligned} \left| F_\eta^N(\nu_N^\theta) - \tilde{F}_\eta^N(\nu_N^\theta) \right| &\leq \frac{L_\ell}{2N^2} \sum_{i=1}^p \int \left\| \sum_{j=1}^N \phi(\theta_j, z_j, x_i) - \tilde{\phi}(\theta_j, x_i) \right\|^2 d\gamma^{\otimes N}(z) \\ &\leq \frac{L_\ell}{2N^2} \sum_{i=1}^p \sum_{j=1}^N \int \left\| \phi(\theta_j, z_j, x_i) - \tilde{\phi}(\theta_j, x_i) \right\|^2 d\gamma(z) . \end{aligned}$$

The proof follows from A1-(ii). \square

We can also show that minimization of F_η^N over $\mathcal{P}_N(\Xi^N)$ provides a good approximation for the minimization problem corresponding to \tilde{F}_η^N for sufficiently large N .

Theorem 4. Assume A1 and that there exists $\nu_\star \in \mathcal{P}(\Xi)$ such that $\nu_\star \in \arg\max_{\mathcal{P}(\Xi)} \tilde{F}_\eta^N$. Suppose in addition that there exists $C_\phi^{\nu_\star} \geq 0$ such that for any $x \in \mathbf{X}$,

$$\int \left\| \tilde{\phi}(\theta, x) - \int \tilde{\phi}(\theta', x) d\nu_\star(\theta') \right\|^2 d\nu_\star(\theta) \leq C_\phi^{\nu_\star} . \quad (15)$$

Then, there exists $C \geq 0$ such that for any $N, p \in \mathbb{N}^*$, $\{(x_i, y_i)\}_{i=1}^p \in (\mathbf{X} \times \mathbf{Y})^p$ and $\eta_N > 0$,

$$\left| \sup_{\theta \in \Xi^N} \text{ELBO}_\eta^N(\theta) - \sup_{\nu \in \mathcal{P}(\Xi)} \tilde{F}_\eta^N(\nu) \right| \leq Cp/N .$$

Proof. Using Theorem 3, we easily get that for any $\theta \in \Xi^N$,

$$\text{ELBO}_\eta^N(\theta) \leq \tilde{F}_\eta^N(\nu_N^\theta) + Cp/N \leq \sup_\nu \tilde{F}_\eta^N(\nu) + Cp/N ,$$

for some $C \geq 0$ independent of $\{(x_i, y_i)\}_{i=1}^p \in (\mathsf{X} \times \mathsf{Y})^p$ and $\eta_N > 0$. On the other hand, we have using ν_\star is a maximizer of \tilde{F}_η^N ,

$$\begin{aligned} \sup_{\theta \in \Xi^N} \text{ELBO}_\eta^N(\theta) &\geq \\ \sup_\nu \tilde{F}_\eta^N(\nu) - \int \left| \text{ELBO}_\eta^N(\theta) - \tilde{F}_\eta^N(\nu_N^\theta) \right| d\nu_\star^{\otimes N}(\theta) &- \int \left| \tilde{F}_\eta^N(\nu_N^\theta) - \tilde{F}_\eta^N(\nu_\star) \right| d\nu_\star^{\otimes N}(\theta) . \end{aligned} \quad (16)$$

Using A1, for any $y \in \mathsf{Y}$, $\tilde{y} \mapsto \ell(y, \tilde{y})$ is L_ℓ -smooth, we get by (Nesterov, 2004, Lemma 1.2.3),

$$\begin{aligned} \int \left| \tilde{F}_\eta^N(\nu_N^\theta) - \tilde{F}_\eta^N(\nu_\star) \right| d\nu_\star^{\otimes N}(\theta) &\leq L_\ell \sum_{i=1}^p \int \left\| \frac{1}{N} \sum_{j=1}^N \tilde{\phi}(\theta_j, x_i) - \int \tilde{\phi}(\theta', x_i) d\nu_\star(\theta') \right\|^2 d\nu_\star^{\otimes N}(\theta) \\ &\leq L_\ell p C_\phi^{\nu_\star} / N . \end{aligned} \quad (17)$$

Combining (16), (17) and Theorem 3 completes the proof. \square

We now set $\eta_N = \tau p/N$ with $\tau > 0$. With this particular choice, \tilde{F}_η^N depends only on the number of observations p but no longer on the number of neurons N . We denote, for that particular choice of η_N ,

$$F_\tau^p(\nu) = p^{-1} \tilde{F}_\eta^N(\nu) = -\frac{1}{p} \sum_{i=1}^p \tilde{G}(\nu; (x_i, y_i)) - \tau \int \text{KL}(q_\theta^1 | P_0^1) d\nu(\theta) .$$

In our next result, we show that with high probability, $F_\tau^p(\nu)$ provides a good approximation of the function

$$R_\tau(\nu) = - \int \tilde{G}(\nu; (x, y)) d\pi(x, y) - \tau \int \text{KL}(q_\theta^1 | P_0^1) d\nu(\theta) , \quad (18)$$

where \tilde{G} is defined by (14). The first term is an integrated log-likelihood with respect to the joint distribution of observations. The second term is a form of penalization of the complexity of ν . It is interesting to note that this penalty term is defined from the prior P_0 and the variational family \mathcal{F}_Θ .

Proposition 5. Assume A1 and that there exists $M_G > 0$, s.t. for any $\nu \in \mathcal{P}(\Xi)$, $0 \leq \tilde{G}(\nu; (x, y)) \leq M_G$, for π -almost all $(x, y) \in \mathsf{X} \times \mathsf{Y}$. Suppose in addition that $\{(x_i, y_i)\}_{i=1}^p$ are i.i.d. with distribution π . Then, for any $\nu \in \mathcal{P}(\Xi)$ and $\delta > 0$, with probability $1 - \delta$ at least, it holds

$$|F_\tau^p(\nu) - R_\tau(\nu)| \leq M_G \sqrt{\log(\delta/2)/(2p)} .$$

The proof follows from applying Hoeffding's inequality on the bounded i.i.d. variables $\tilde{G}(\nu; (x_i, y_i))$ for $i = 1, \dots, p$.

It is worth noting that this limiting risk is similar to the one obtained in the analysis of the limiting behavior of gradient descent type algorithms for one or two hidden layers in the overparameterized regime, by Chizat and Bach (2018); Rotskoff et al. (2019); Mei et al. (2018); Tzen and Raginsky (2019); De Bortoli et al. (2020) - see (1). Moreover, the maximization of the ELBO using gradient descent can be viewed as a temporal and spatial discretization of the Wasserstein gradient flow of the limiting function (18).

For simplicity, we illustrate our result for a mean-field variational family associated with the family of C^1 -diffeomorphisms on \mathbb{R}^d , $\{\mathcal{T}_\theta : \theta \in \Xi\}$ given in (8) for $\Xi \subset \mathbb{R}^d \times (\mathbb{R}_+^*)^d$. Consider the following assumption.

A2. (i) The subset Ξ is a compact set of $\mathbb{R}^d \times (\mathbb{R}_+^*)^d$, and X, Y are compact sets of $\mathbb{R}^{d_x}, \mathbb{R}^{d_y}$.

(ii) The probability measure γ satisfies $\int \|z\|^4 d\gamma(z) < +\infty$.

(iii) For any $x \in \mathsf{X}$, there exists $L_h \geq 0$ such that the function $b \mapsto h(b, x)$ is L_h -Lipschitz on \mathbb{R}^{d_x} and $\sup_{x \in \mathsf{X}, b \in \mathbb{R}^{d_x}} |h(b, x)| / (1 + \|b\|) < +\infty$.

(iv) The prior density P_0^1 is positive on \mathbb{R}^d and satisfies $\theta \mapsto \text{KL}(q_\theta^1|P_0^1)$ is continuous on Ξ .

Note that the condition that for any $x \in \mathbf{X}$, the condition $b \mapsto h(b, x)$ is L_h -Lipschitz is automatically satisfied for h of the form (2) with σ the RELU or sigmoid function if \mathbf{X} is bounded. Also, we verify in the next proposition that $\theta \mapsto \text{KL}(q_\theta^1|P_0^1)$ is continuous if P_0^1 and γ are non-degenerate Gaussian distributions.

Proposition 6. Assume A1-(i) and A2. Then A1-(ii) and the conditions of Theorem 4 hold.

Proof. We first prove A1-(ii). Recall, that for $\theta, z, x \in \Xi \times \mathbb{R}^d \times \mathbf{X}$, $\phi(\theta, z, x) = s(\mathcal{T}_\theta(z), x)$ where $\mathcal{T}_\theta(z) = \mu + \sigma \odot z$. Therefore, by (3), decomposing each weight as $w = (a, b)$ where a is the output weight and b is the hidden weight, $\phi(\theta, z, x) = ah(b, x)$, with $a = \mu_a + \sigma_a \odot z_a$ and $b = \mu_b + \sigma_b \odot z_b$, $\theta = (\theta_a, \theta_b)$, $\theta_a = (\mu_a, \sigma_a) \in \mathbb{R}^{d_Y} \times (\mathbb{R}_+^*)^{d_Y}$ and $\theta_b = (\mu_b, \sigma_b) \in \mathbb{R}^{d_X} \times (\mathbb{R}_+^*)^{d_X}$. Hence,

$$\|a\|^2 \leq 2\|\mu_a\|^2 + 2\|\sigma_a\|^2\|z_a\|^2 \leq 2\|\theta\|^2(1 + \|z_a\|^2), \quad \|b\|^2 \leq 2\|\theta\|^2(1 + \|z_b\|^2).$$

Also, by A2, there exist $C_0, C_1 \geq 0$ such that for any x, b , $|h(b, x)| \leq C_0 + C_1\|b\|$. Hence, we have for any $\theta \in \Xi$, $z \in \mathbb{R}^d$ and $x \in \mathbf{X}$,

$$\begin{aligned} \|\phi(\theta, z, x)\|^2 &\leq \|a\|^2(C_0 + C_1\|b\|)^2 \\ &\leq 2\|\theta\|^2(1 + \|z_a\|^2)[C_0 + 2C_1\|\theta\|(1 + \|z_b\|)^{\frac{1}{2}}]^2 \leq C_3(1 + \|z\|^4)(1 + \|\theta\|^2), \end{aligned} \quad (19)$$

for some constant $C_3 > 0$. As Ξ is compact and $\int \|z\|^4 d\gamma(z) < +\infty$, it follows that A1-(ii) holds. We now show that $\arg\max_{\mathcal{P}(\Xi)} \tilde{F}_\eta^N \neq \emptyset$. By Lemma 7 in the supplement, $\tilde{\phi}$ is bounded and for any $x \in \mathbf{X}$, $\theta \mapsto \tilde{\phi}(\theta, x)$ is continuous. Using that under A2 for any $y \in \mathbf{Y}$, $\tilde{y} \mapsto \ell(y, \tilde{y})$ is continuous, it follows that $\nu \mapsto \tilde{G}(\nu; (x, y))$ is continuous for the weak topology on $\mathcal{P}(\Xi)$ for any $(x, y) \in \mathbf{X} \times \mathbf{Y}$. In addition, since $\theta \mapsto \text{KL}(q_\theta^1|P_0)$ is continuous, we get since Ξ is compact that $\nu \mapsto \int \text{KL}(q_\theta^1|P_0^1) d\nu(\theta)$ is continuous for the weak topology. It follows that $\nu \mapsto \tilde{F}_\eta^N(\nu)$ is continuous for the weak topology. Using Ξ is compact, $\mathcal{P}(\Xi)$ is compact for the weak topology by Ambrosio et al. (2008, Theorem 5.1.3), and it follows that $\arg\max_{\mathcal{P}(\Xi)} \tilde{F}_\eta^N \neq \emptyset$. The last condition (15) of Theorem 4 easily follows from Lemma 7. \square

4 Experiments

In this section we illustrate our findings and their practical implications for image classification on standard datasets (MNIST, CIFAR-10). The reader may refer to Appendix C for additional experiments, including on regression tasks, that highlight the importance of rescaling the ELBO. Our code is available at https://github.com/THuix/bnn_mfvi. In this section, we illustrate the influence of the parameter τ through different metrics.

Evaluation. Let $\mathcal{D} = (x_i, y_i)_{i=1}^p$ be a dataset, where $y_i = c \in \{1, \dots, n_l\}$ is a discrete class label. For an input $x \in \mathbf{X}$, the predictive probability of a class c by a neural network with weights \bar{w} is defined by $\Psi_c(f_{\bar{w}}(x))$, where $\Psi_c(f_{\bar{w}}(x))$ denotes the c -th component of the softmax function applied to the output $f_{\bar{w}}(x) \in \mathbb{R}^{n_l}$ of the neural network. The cross entropy loss writes $\ell_{\text{CE}}(y, f_{\bar{w}}(x)) = -\sum_{c=1}^{n_l} \tilde{y}_c \log(\Psi_c(f_{\bar{w}}(x)))$, where \tilde{y}_c denotes the c -th coordinate of a one-hot representation of the label y and the Negative Log Likelihood (NLL) $\sum_{i=1}^p \int_{\mathbb{R}^{N \times d}} \ell_{\text{CE}}(y_i, f_{\bar{w}}(x_i)) q_{\theta}(\bar{w}) d\text{Leb}_{d \times N}(\bar{w})$. The calibration performance of the model can be estimated by the Expected Calibration Error (ECE) Naeini et al. (2015), see also Appendix C.2. We recall that model is calibrated if the predictive posterior is the true probability for each class $c \in \{1, \dots, n_l\}$. However, since these probabilities are unknown, they have to be estimated, e.g. through ECE. As the NLL, ECE penalizes low probabilities assigned to correct predictions and high probabilities assigned to wrong ones; but these evaluation metrics are not strictly equivalent. To make our prediction, for $x \in \mathbf{X}$, we use the posterior predictive distribution defined for a class c as $\int \Psi_c(f_{\bar{w}}(x)) q_{\theta^*}(\bar{w}) d\text{Leb}_{d \times N}(\bar{w})$ with θ^* obtained by minimization of ELBO_η^N by Bayes by Backprop. This integral is estimated by an empirical version

$$\int \Psi_c(f_{\bar{w}}(x)) q_{\theta^*}(\bar{w}) d\text{Leb}_{d \times N}(\bar{w}) \approx \frac{1}{m} \sum_{l=1}^m \Psi_c(f_{\bar{w}_l}(x)), \quad (20)$$

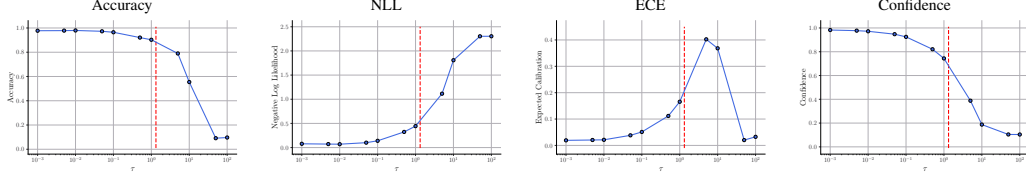


Figure 1: Effect of the temperature for a Linear BNN trained on MNIST. No cooling $\eta_N = 1$ is indicated by a red line.

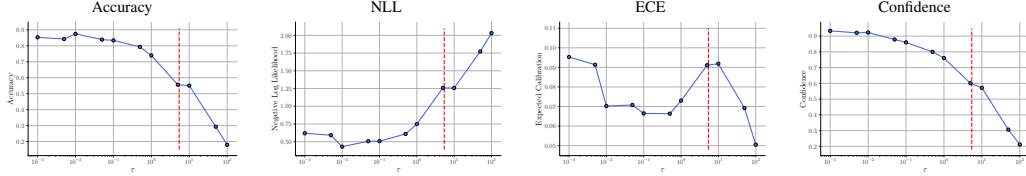


Figure 2: Effect of the temperature for a Resnet20 trained on CIFAR-10. No cooling $\eta_N = 1$ is indicated by a red line.

where for $l = 1, \dots, m$, \tilde{w}_l are i.i.d. samples from $q\theta^*$. All the evaluation metrics mentioned above (NLL, ECE), as well as the accuracy are estimated using the same procedure. We will present our results on the MNIST dataset (where $p = 6 \cdot 10^4$) and the CIFAR-10 dataset (where $p = 5 \cdot 10^4$) [Krizhevsky et al. \(2009\)](#).

Setup. We use a Linear BNN on MNIST, and ResNet20 architecture [He et al. \(2016\)](#) on CIFAR-10 [Simonyan and Zisserman \(2014\)](#). For CIFAR-10, we use the standard data augmentation techniques, see [Khan et al. \(2018\)](#). For each neuron, we use a centered Gaussian prior with variance $1/5$, following [Osawa et al. \(2019\)](#). We train each BNN by Bayes by Backprop [Blundell et al. \(2015\)](#) with the reparametrization trick (see Appendix D) and using batch normalization [Sergey and Christian \(2021\)](#).

Figure 1, 2 illustrate the performance of the different models and data sets for different values of τ . We evaluate the models on the test set in terms of their accuracy, NLL, ECE, and average confidence over the test set. In all experiments, we take $m = 50$ in (20) to approximate a BNN prediction and average our results over 5 experiments for each τ . It is worth noting that for a large τ , the accuracy decreases while the NLL increases. This is hardly a surprise, since the KL regularization forces the VI posterior to stay close to the prior distribution, resulting in underfitting. At the same time, the ECE value is low because of the poor confidence in the model, which is reflected in the accuracy. For small values of τ , the data fitting term is privileged, so the accuracy of the model is high, while the NLL is low. At the same time, the confidence in the model is very high, resulting in a low ECE. For intermediate values of τ , the accuracy of the models starts to decrease, but slower than the confidence in the model, which explains an increase in ECE. We also illustrate the different regimes for the parameter τ with additional experiments in Appendix C, including analysis of the weights distribution and out-of-distribution detection.

5 Conclusion

In this work, we studied BNN trained with mean-field VI in the overparameterized regime. We have highlighted both theoretically and numerically that the partially tempered ELBO_η^N advocated for VI for BNN effectively addresses the potential imbalance between the data fitting and KL terms. For mean-field VI and product prior distributions, we found that the cooling parameter must be chosen proportional to the ratio between the number of observations and neurons to achieve a balance between the data fitting and KL regularizer. With this choice, ELBO_η^N converges to a limiting functional that has the same structure as the one given by [Chizat and Bach \(2018\)](#); [Rotskoff et al. \(2019\)](#); [Mei et al. \(2018\)](#); [Tzen and Raginsky \(2019\)](#); [De Bortoli et al. \(2020\)](#) for empirical risk minimization. We also explained why, in the absence of cooling, the KL term can dominate the

data fitting term, typically leading to underfitting of the model, which in practice translates into poor results on all metrics considered. Our work therefore provides a well-grounded theoretical justification for the importance of using a partial tempering in the overparameterized framework, which completes the justifications given by [Wenzel et al. \(2020\)](#); [Izmailov et al. \(2021\)](#); [Nabarro et al. \(2021\)](#); [Noci et al. \(2021\)](#); [Laves et al. \(2021\)](#). While our theoretical results apply to a neural network with a single hidden layer, we have shown numerically that similar conclusions can be drawn for more general NN architectures. We emphasize that the introduction of a cooling factor into the Mean-Field VI for BNN is not without implications for the validity of Bayesian inference, and that the conclusions that can be drawn in this framework-in particular, Bayesian uncertainty quantification-must therefore be used with care (even though the accuracy, NLL, and ECE metrics obtained with Mean-Field VI compare favorably to their "classical" ERM learning counterparts).

References

- Ambrosio, L., Gigli, N., and Savaré, G. (2008). *Gradient flows: in metric spaces and in the space of probability measures*. Springer Science & Business Media.
- Ashukha, A., Lyzhov, A., Molchanov, D., and Vetrov, D. (2020). Pitfalls of in-domain uncertainty estimation and ensembling in deep learning. *arXiv preprint arXiv:2002.06470*.
- Barron, A. R. and Cover, T. M. (1991). Minimum complexity density estimation. *IEEE transactions on information theory*, 37(4):1034–1054.
- Betancourt, M. (2017). A conceptual introduction to hamiltonian monte carlo. *arXiv preprint arXiv:1701.02434*.
- Bhattacharya, A., Pati, D., and Yang, Y. (2019). Bayesian fractional posteriors. *The Annals of Statistics*, 47(1):39–66.
- Blei, D. M., Kucukelbir, A., and McAuliffe, J. D. (2017). Variational inference: A review for statisticians. *Journal of the American statistical Association*, 112(518):859–877.
- Blundell, C., Cornebise, J., Kavukcuoglu, K., and Wierstra, D. (2015). Weight uncertainty in neural network. In *International Conference on Machine Learning*, pages 1613–1622. PMLR.
- Brosse, N., Durmus, A., and Moulines, E. (2018). The promises and pitfalls of stochastic gradient langevin dynamics. In *NeurIPS*.
- Chen, T., Fox, E., and Guestrin, C. (2014). Stochastic gradient hamiltonian monte carlo. In *International conference on machine learning*, pages 1683–1691. PMLR.
- Chizat, L. and Bach, F. (2018). On the global convergence of gradient descent for over-parameterized models using optimal transport. *arXiv preprint arXiv:1805.09545*.
- Cobb, A. D. and Jalaian, B. (2021). Scaling hamiltonian monte carlo inference for bayesian neural networks with symmetric splitting. In *Uncertainty in Artificial Intelligence*, pages 675–685. PMLR.
- Coker, B., Pan, W., and Doshi-Velez, F. (2021). Wide mean-field variational bayesian neural networks ignore the data. *arXiv preprint arXiv:2106.07052*.
- De Bortoli, V., Durmus, A., Fontaine, X., and Simsekli, U. (2020). Quantitative propagation of chaos for sgd in wide neural networks. *arXiv preprint arXiv:2007.06352*.
- Farquhar, S., Osborne, M., and Gal, Y. (2019). Radial bayesian neural networks: Robust variational inference in big models. *Training*, 80:100.
- Filos, A., Farquhar, S., Gomez, A. N., Rudner, T. G., Kenton, Z., Smith, L., Alizadeh, M., De Kroon, A., and Gal, Y. (2019). A systematic comparison of bayesian deep learning robustness in diabetic retinopathy tasks. *arXiv preprint arXiv:1912.10481*.
- Fortuin, V. (2021). Priors in bayesian deep learning: A review. *arXiv preprint arXiv:2105.06868*.

- Fortuin, V., Garriga-Alonso, A., Wenzel, F., Rätsch, G., Turner, R., van der Wilk, M., and Aitchison, L. (2021). Bayesian neural network priors revisited. *arXiv preprint arXiv:2102.06571*.
- Gal, Y. and Ghahramani, Z. (2016). Dropout as a bayesian approximation: Representing model uncertainty in deep learning. In *international conference on machine learning*, pages 1050–1059. PMLR.
- Graves, A. (2011). Practical variational inference for neural networks. *Advances in neural information processing systems*, 24.
- Grünwald, P. (2012). The safe bayesian. In *International Conference on Algorithmic Learning Theory*, pages 169–183. Springer.
- Grunwald, P., Steinke, T., and Zakynthinou, L. (2021). Pac-bayes, mac-bayes and conditional mutual information: Fast rate bounds that handle general vc classes. In Belkin, M. and Kpotufe, S., editors, *Proceedings of Thirty Fourth Conference on Learning Theory*, volume 134 of *Proceedings of Machine Learning Research*, pages 2217–2247. PMLR.
- Grünwald, P. and Van Ommen, T. (2017). Inconsistency of bayesian inference for misspecified linear models, and a proposal for repairing it. *Bayesian Analysis*, 12(4):1069–1103.
- He, K., Zhang, X., Ren, S., and Sun, J. (2016). Deep residual learning for image recognition. In *Proceedings of the IEEE conference on computer vision and pattern recognition*, pages 770–778.
- Heide, R., Kirichenko, A., Grunwald, P., and Mehta, N. (2020). Safe-bayesian generalized linear regression. In *International Conference on Artificial Intelligence and Statistics*, pages 2623–2633. PMLR.
- Hernández-Lobato, J. M. and Adams, R. (2015). Probabilistic backpropagation for scalable learning of bayesian neural networks. In *International conference on machine learning*, pages 1861–1869. PMLR.
- Hoffman, M. D., Gelman, A., et al. (2014). The no-u-turn sampler: adaptively setting path lengths in hamiltonian monte carlo. *J. Mach. Learn. Res.*, 15(1):1593–1623.
- Izmailov, P., Vikram, S., Hoffman, M. D., and Wilson, A. G. (2021). What are bayesian neural network posteriors really like? *International Conference on Machine Learning*.
- Jospin, L. V., Buntine, W., Boussaid, F., Laga, H., and Bennamoun, M. (2020). Hands-on bayesian neural networks—a tutorial for deep learning users. *arXiv preprint arXiv:2007.06823*.
- Kendall, A. and Gal, Y. (2017). What uncertainties do we need in bayesian deep learning for computer vision? *arXiv preprint arXiv:1703.04977*.
- Khan, M., Nielsen, D., Tangkaratt, V., Lin, W., Gal, Y., and Srivastava, A. (2018). Fast and scalable bayesian deep learning by weight-perturbation in adam. In *International Conference on Machine Learning*, pages 2611–2620. PMLR.
- Khan, M. E. and Rue, H. (2021). The bayesian learning rule. *arXiv preprint arXiv:2107.04562*.
- Krizhevsky, A., Hinton, G., et al. (2009). Learning multiple layers of features from tiny images.
- Laves, M.-H., Tölle, M., Schlaefel, A., and Engelhardt, S. (2021). Posterior temperature optimization in variational inference for inverse problems. *arXiv preprint arXiv:2106.07533*.
- Louizos, C. and Welling, M. (2017). Multiplicative normalizing flows for variational bayesian neural networks. In *International Conference on Machine Learning*, pages 2218–2227. PMLR.
- McAllister, R., Gal, Y., Kendall, A., van der Wilk, M., Shah, A., Cipolla, R., and Weller, A. (2017). Concrete problems for autonomous vehicle safety: Advantages of bayesian deep learning. In *IJCAI*.
- Mei, S., Montanari, A., and Nguyen, P.-M. (2018). A mean field view of the landscape of two-layer neural networks. *Proceedings of the National Academy of Sciences*, 115(33):E7665–E7671.

- Michelmores, R., Wicker, M., Laurenti, L., Cardelli, L., Gal, Y., and Kwiatkowska, M. (2020). Uncertainty quantification with statistical guarantees in end-to-end autonomous driving control. In *2020 IEEE International Conference on Robotics and Automation (ICRA)*, pages 7344–7350. IEEE.
- Nabarro, S., Ganev, S., Garriga-Alonso, A., Fortuin, V., van der Wilk, M., and Aitchison, L. (2021). Data augmentation in bayesian neural networks and the cold posterior effect. *arXiv preprint arXiv:2106.05586*.
- Naeini, M. P., Cooper, G., and Hauskrecht, M. (2015). Obtaining well calibrated probabilities using bayesian binning. In *Twenty-Ninth AAAI Conference on Artificial Intelligence*.
- Neal, R. M. et al. (2011). Mcmc using hamiltonian dynamics. *Handbook of markov chain monte carlo*, 2(11):2.
- Nesterov, Y. (2004). *Introductory Lectures on Convex Optimization: A Basic Course*. Applied Optimization. Springer.
- Netzer, Y., Wang, T., Coates, A., Bissacco, A., Wu, B., and Ng, A. Y. (2011). Reading digits in natural images with unsupervised feature learning.
- Noci, L., Roth, K., Bachmann, G., Nowozin, S., and Hofmann, T. (2021). Disentangling the roles of curation, data-augmentation and the prior in the cold posterior effect. *arXiv preprint arXiv:2106.06596*.
- Ober, S. W. and Aitchison, L. (2021). Global inducing point variational posteriors for bayesian neural networks and deep gaussian processes. In *International Conference on Machine Learning*, pages 8248–8259. PMLR.
- Osawa, K., Swaroop, S., Jain, A., Eschenhagen, R., Turner, R. E., Yokota, R., and Khan, M. E. (2019). Practical deep learning with bayesian principles. *arXiv preprint arXiv:1906.02506*.
- Rotskoff, G., Jelassi, S., Bruna, J., and Vanden-Eijnden, E. (2019). Global convergence of neuron birth-death dynamics. *arXiv preprint arXiv:1902.01843*.
- Sergey, I. and Christian, S. (2021). Batch normalization: Accelerating deep network training by reducing internal covariate shift. *arxiv 2015. arXiv preprint arXiv:1502.03167*.
- Simonyan, K. and Zisserman, A. (2014). Very deep convolutional networks for large-scale image recognition. *arXiv preprint arXiv:1409.1556*.
- Sun, S., Zhang, G., Shi, J., and Grosse, R. (2019). Functional variational bayesian neural networks. In *International Conference on Learning Representations*.
- Tran, B.-H., Rossi, S., Milios, D., and Filippone, M. (2020). All you need is a good functional prior for bayesian deep learning. *arXiv preprint arXiv:2011.12829*.
- Tzen, B. and Raginsky, M. (2019). Neural stochastic differential equations: Deep latent gaussian models in the diffusion limit. *arXiv preprint arXiv:1905.09883*.
- Welling, M. and Teh, Y. W. (2011). Bayesian learning via stochastic gradient langevin dynamics. In *International conference on machine learning*, pages 681–688. Citeseer.
- Wenzel, F., Roth, K., Veeling, B. S., Swiatkowski, J., Tran, L., Mandt, S., Snoek, J., Salimans, T., Jenatton, R., and Nowozin, S. (2020). How good is the bayes posterior in deep neural networks really? *International conference on machine learning*.
- Wilson, A. G. and Izmailov, P. (2020). Bayesian deep learning and a probabilistic perspective of generalization. *arXiv preprint arXiv:2002.08791*.
- Zhang, G., Sun, S., Duvenaud, D., and Grosse, R. (2018). Noisy natural gradient as variational inference. In *International Conference on Machine Learning*, pages 5852–5861. PMLR.
- Zhang, T. (2006). Information-theoretic upper and lower bounds for statistical estimation. *IEEE Transactions on Information Theory*, 52(4):1307–1321.

A Technical result

Lemma 7. Assume A1-(i) and A2. Then for any $x \in \mathsf{X}$, the function $\theta \mapsto \tilde{\phi}(\theta, x)$ is continuous. In addition, there exists $C \geq 0$ such that for any $x \in \mathsf{X}$ and $\theta \in \Xi$, $\|\tilde{\phi}(\theta, x)\| \leq C$.

Proof. Since $\phi(\theta, z, x) = ah(b, x)$ and since by A2, $b \mapsto h(b, x)$ is continuous for any $x \in \mathsf{X}$, it follows that for any $x \in \mathsf{X}$, $z \in \mathbb{R}^d$, $\theta \mapsto \phi(\theta, z, x)$ is continuous on Ξ . Using (19) and the condition that Ξ is compact, an application of the Lebesgue dominated convergence theorem implies that for any $x \in \mathsf{X}$, the function $\theta \mapsto \tilde{\phi}(\theta, x)$ is continuous. Finally, Eq. (19) and the condition that Ξ is compact shows that there exists $C \geq 0$ such that for any $x \in \mathsf{X}$ and $\theta \in \Xi$, $\|\tilde{\phi}(\theta, x)\| \leq C$. \square

B Proof of Proposition 1

We have assumed that \mathcal{F}_Θ is a family of Gaussians with diagonal covariance matrices, and that $P_0 \in \mathcal{F}_\Theta$ hence there exists $\theta_0 = (\mu, \sigma) \in \mathbb{R}^{N(d_X+d_Y)} \times \mathbb{R}^{N(d_X+d_Y)}$ such that $P_0 = q_{\theta_0}$. For ease of notations, we work with P_0 standard Gaussian:

$$P_0(\bar{w}) = \prod_{j=1}^N \prod_{l=1}^{d_Y} \mathcal{N}(a_{j,l}; 0, 1) \times \prod_{j=1}^N \prod_{l=1}^{d_X} \mathcal{N}(b_{j,l}; 0, 1) \quad (21)$$

Our results hold for more general parameters for P_0 but we fix these ones for convenience of notations. The posterior $q_\theta \in \mathcal{F}_\Theta$ is:

$$q_\theta(\bar{w}) = \prod_{j=1}^N \prod_{l=1}^{d_Y} \mathcal{N}(a_{j,l}; \mu_{a_{j,l}}, \sigma_{a_{j,l}}^2) \times \prod_{j=1}^N \prod_{l=1}^{d_X} \mathcal{N}(b_{j,l}; \mu_{b_{j,l}}, \sigma_{b_{j,l}}^2) \quad (22)$$

We define $a_j = (a_{j,1}, \dots, a_{j,d_Y}) \in \mathbb{R}^{d_Y}$ and $b_j = (b_{1,j}, \dots, b_{d_X,j}) \in \mathbb{R}^{d_X}$ respectively the j^{th} row of the first layer weight matrix and the j^{th} column of the second layer weight matrix. We denote $\mu_{a_j} = (\mu_{a_{j,1}}, \dots, \mu_{a_{j,d_Y}}) \in \mathbb{R}^{d_Y}$, $\mu_a = (\mu_{a_1}, \dots, \mu_{a_N}) \in \mathbb{R}^{Nd_Y}$.

Recall that

$$\text{ELBO}^N(\theta) = -\mathcal{L}(q_\theta) - \text{KL}(q_\theta | q_{\theta_0}), \quad \text{with } \mathcal{L}(q_\theta) = -\mathbb{E}_{\bar{w} \sim q_\theta} \left[\sum_{i=1}^p \log(L(y_i | x_i, \bar{w})) \right], \quad (23)$$

where $L(y | x, \bar{w}) \propto \exp(-\ell(f_{\bar{w}}(x), y))$ is defined by (4).

By the optimality of θ^* , we have:

$$\text{ELBO}^N(\theta^*) \geq \text{ELBO}^N(\theta_0),$$

Hence,

$$\text{KL}(q_{\theta^*} | q_{\theta_0}) \leq \mathcal{L}(q_{\theta_0}) - \mathcal{L}(q_{\theta^*}). \quad (24)$$

We now deal separately with the square loss (Case 1) and cross-entropy loss (Case 2). Throughout, we will often use the notation $\sigma_j = \sigma(\langle b_j, x \rangle)$ for any $j = 1, \dots, N$ and a generic point $x \in \mathsf{X}$. Since we have assumed that σ is L -Lipschitz, for any $y \in \mathbb{R}$, $|\sigma(y)| \leq |\sigma(0)| + L|y|$. Also, to explicit the dependence of θ^* , θ_0 in N we will write their associated distributions $q_{\theta^*}^N$ and $q_{\theta_0}^N$ respectively.

B.1 Case of the square loss

Proof. The idea of the proof is to show that the right hand side term of (24) converges to zero by showing that the two negative log likelihoods converge to the same finite limit, and hence their difference to zero as N goes to infinity. When l is the square loss, for any $q_\theta^N \in \mathcal{F}_\Theta$, by (23) we have

$$\mathcal{L}(q_\theta^N) = \sum_{i=1}^p \mathbb{E}_{\bar{w} \sim q_\theta^N} [\|y_i\|^2 + \|f_{\bar{w}}(x_i)\|^2 - 2\langle y_i, f_{\bar{w}}(x_i) \rangle + \log(Z)],$$

where Z is the normalization constant of the model defined by (4). We will show that for both the prior $q_{\theta_0}^N$ and optimal posterior $q_{\theta^*}^N$, the first and second moment of the predictive distribution converge to zero as N goes to infinity.

Under the prior distribution (21), for any $x \in \mathbb{X}$, the first and second moments of the predictive distribution can be written:

$$\begin{aligned}\mathbb{E}_{\bar{w} \sim q_{\theta_0}^N}[f_{\bar{w}}(x)] &= \mathbb{E}\left[\frac{1}{N} \sum_{j=1}^N \sigma_j a_j\right] = \frac{1}{N} \sum_{j=1}^N \mathbb{E}[\sigma_j] \mathbb{E}[a_j] = 0 \\ \mathbb{E}_{\bar{w} \sim q_{\theta_0}^N}[\|f_{\bar{w}}(x)\|^2] &= \mathbb{E}_{\bar{w} \sim q_{\theta_0}^N}\left[\frac{1}{N^2} \left(\sum_{j=1}^N \sigma_j^2 \|a_j\|^2 + 2 \sum_{j=1}^N \sum_{k < j} \sigma_j \sigma_k \langle a_j, a_k \rangle\right)\right] \\ &= \frac{1}{N^2} \sum_{j=1}^N \mathbb{E}_{\bar{w} \sim q_{\theta_0}^N}[\sigma_j^2] \leq \frac{1}{N^2} \left(\sum_{j=1}^N |\sigma(0)|^2 + L^2 \|x\|^2 \mathbb{E}_{\bar{w} \sim q_{\theta_0}^N}[\|b_j\|^2]\right) \\ &\xrightarrow{N \rightarrow \infty} 0,\end{aligned}$$

Hence we first obtain:

$$\lim_{N \rightarrow \infty} \mathcal{L}(q_{\theta_0}^N) = \sum_{i=1}^p \|y_i\|^2 + \log Z. \quad (25)$$

We now turn to showing that $\mathcal{L}(q_{\theta^*}^N)$ has the same limit. First notice that since \mathcal{L} is a positive function, by (24) we have: $\text{KL}(q_{\theta^*}^N | q_{\theta_0}^N) \leq \mathcal{L}(q_{\theta_0}^N)$. Since the right-hand term is a converging sequence, it means that $\text{KL}(q_{\theta^*}^N | q_{\theta_0}^N)$ is bounded by a constant C_{KL} independent of N .

By applying Lemma 8 and Lemma 9, we have:

$$\begin{aligned}\mathbb{E}_{\bar{w} \sim q_{\theta^*}^N}[\langle y_i, f_{\bar{w}}(x_i) \rangle] &\leq \|y_i\| \|\mathbb{E}_{\bar{w} \sim q_{\theta^*}^N}[f_{\bar{w}}(x_i)]\| \leq \frac{\phi(\text{KL}(q_{\theta^*}^N, q_{\theta_0}^N), \mathbb{X}, d_Y)}{\sqrt{N}} \leq \frac{\phi(C_{\text{KL}}, \mathbb{X}, d_Y)}{\sqrt{N}} \\ \mathbb{E}_{\bar{w} \sim q_{\theta^*}^N}[\|f_{\bar{w}}(x)\|^2] &\leq \frac{\psi(\text{KL}(q_{\theta^*}^N, q_{\theta_0}^N), \mathbb{X}, d_Y)}{\sqrt{N}} \leq \frac{\psi(C_{\text{KL}}, \mathbb{X}, d_Y)}{\sqrt{N}}\end{aligned}$$

where the most right hand side inequalities come from the fact that $\text{KL}(q_{\theta^*}^N | q_{\theta_0}^N)$ is bounded by a constant C_{KL} independent of N ; and $\phi(C_{\text{KL}}, \mathbb{X}, d_Y), \psi(C_{\text{KL}}, \mathbb{X}, d_Y)$ are constants that only depend on the data points $(x_i, y_i)_{i=1}^p$, the spaces \mathbb{X}, \mathbb{Y} and parameters of the prior distribution (through C_{KL}). Hence, the first and second moments of the predictive under the posterior $q_{\theta^*}^N$ converge to 0. Hence, we obtain:

$$\lim_{N \rightarrow \infty} \mathcal{L}(q_{\theta^*}^N) = \sum_{i=1}^p \|y_i\|^2 + \log Z. \quad (26)$$

From (24), (25) and (26) we finally that

$$\lim_{N \rightarrow \infty} \text{KL}(q_{\theta^*}^N, q_{\theta_0}^N) = 0.$$

B.2 Case of the cross-entropy

Proof. Similarly to the square loss case, the idea of the proof is to show that $\mathcal{L}(q_{\theta_0}^N), \mathcal{L}(q_{\theta^*}^N)$ have the same limit. We will make use of Lemma 10 which specify that limit under a null moment assumption.

Under the prior distribution $q_{\theta_0}^N$,

$$\|\mathbb{E}_{\bar{w} \sim q_{\theta_0}^N}[\frac{1}{N} \sum_{j=1}^N \sigma_j a_j]\| = \frac{1}{N} \|\sum_{j=1}^N \mathbb{E}[\sigma_j] \mathbb{E}[a_j]\| = 0,$$

hence by Lemma 10:

$$\lim_{N \rightarrow \infty} \mathcal{L}(q_{\theta_0}^N) = p(\log(d_Y) + \log Z).$$

We now turn to the predictive distribution under the posterior $q_{\theta^*}^N$. Recall that since \mathcal{L} is a positive function, using the optimality of the posterior we have: $\text{KL}(q_{\theta^*}^N | q_{\theta_0}^N) \leq \mathcal{L}(q_{\theta_0}^N)$. Since the right-hand term is a converging sequence, it means that $\text{KL}(q_{\theta^*}^N | q_{\theta_0}^N)$ is bounded by a constant C_{KL} independent of N .

By Lemma 8, we can bound the first moment of the predictive distribution as:

$$\|\mathbb{E}_{\bar{w} \sim q_{\theta^*}^N}[f_{\bar{w}}(x)]\| \leq \frac{\phi(\text{KL}(q_{\theta^*}^N, q_{\theta_0}^N), \mathbf{X}, d_Y)}{\sqrt{N}} \leq \frac{\phi(C_{\text{KL}}, \mathbf{X}, d_Y)}{\sqrt{N}},$$

where the last inequality comes from the fact that the KL term is bounded by a constant C_{KL} independent of N for the optimal variational parameter $\theta^{*,N}$. Moreover, by using similar argument than in the proof of Lemma 8, we can show that each coordinate μ, σ of $\theta^{*,N}$ is bounded as:

- $\mu \leq \sqrt{2\text{KL}(q_{\theta^*}^N, q_{\theta_0}^N)} \leq \sqrt{2C_{\text{KL}}}$
- $\sigma \leq 2\text{KL}(q_{\theta^*}^N, q_{\theta_0}^N) + 1 \leq 2C_{\text{KL}} + 1$

It means that each neuron weight has bounded mean and variance. We can thus apply Lemma 10, which yields:

$$\lim_{N \rightarrow \infty} \mathcal{L}(q_{\theta}^N) = p(\log(d_Y) - \log Z).$$

As $0 \leq \text{KL}(q_{\theta^*}^N | q_{\theta_0}^N) \leq \mathcal{L}(q_{\theta_0}^N) - \mathcal{L}(q_{\theta^*}^N)$ we obtain:

$$\lim_{N \rightarrow \infty} \text{KL}(q_{\theta^*}^N, q_{\theta_0}^N) = 0.$$

Lemma 8. Assume the conditions of Proposition 1 hold. Then there exists a function ϕ , increasing in its first variable, such that

$$\|\mathbb{E}_{\bar{w} \sim q_{\theta}^N}[f_{\bar{w}}(x)]\| \leq \frac{\phi(\text{KL}(q_{\theta}^N, q_{\theta_0}^N), \mathbf{X}, d_Y)}{\sqrt{N}}.$$

Proof. By Cauchy-Schwartz inequality, the first moment of the predictive distribution under the variational posterior can be upper bounded as:

$$\|\mathbb{E}_{\bar{w} \sim q_{\theta}^N}[f_{\bar{w}}(x)]\| = \frac{1}{N} \|\mathbb{E}_{\bar{w} \sim q_{\theta}^N}[\sum_{j=1}^N \sigma(\langle b_j, x \rangle) a_j]\| \leq \frac{1}{N} \sum_{j=1}^N \|\mathbb{E}[\sigma(\langle b_j, x \rangle)]\| \|\mu_{a_j}\|.$$

Since σ is Lipschitz, $|\sigma(x)| \leq C_0 + L|x|$ where $C_0 = |\sigma(0)|$. Hence,

$$\|\mathbb{E}[\sigma(\langle b_j, x \rangle)]\| \leq |C_0 + L\mathbb{E}[|\langle b_j, x \rangle|]| \leq C_0 + L \sum_{l=1}^{d_X} \mathbb{E}[|b_{j,l}|] |x_l|$$

Let's start by finding an upper bound for $\mathbb{E}[|b_{j,l}|]$. If $b_{j,l} \sim \mathcal{N}(\mu_{b_{j,l}}, \sigma_{b_{j,l}}^2)$, then $|b_{j,l}|$ has an absolute Gaussian distribution and denoting Φ the CDF of a standard Gaussian, we have

$$\mathbb{E}[|b_{j,l}|] = \sigma_{b_{j,l}} \sqrt{\frac{2}{\pi}} \exp\left(\frac{-\mu_{b_{j,l}}^2}{2\sigma_{b_{j,l}}^2}\right) + \mu_{b_{j,l}} \left[1 - 2\Phi\left(\frac{-\mu_{b_{j,l}}}{\sigma_{b_{j,l}}}\right)\right] \leq \sigma_{b_{j,l}} \sqrt{\frac{2}{\pi}} + |\mu_{b_{j,l}}|.$$

Recall that the KL between the posterior q_{θ}^N and prior $q_{\theta_0}^N$ can be written:

$$\begin{aligned} \text{KL}(q_{\theta}^N | q_{\theta_0}^N) = \frac{1}{2} \sum_{j=1}^N \left[\sum_{l=1}^{d_X} (\mu_{b_{j,l}}^2 + \sigma_{b_{j,l}}^2 - \log(\sigma_{b_{j,l}}^2) - 1) \right. \\ \left. + \sum_{l=1}^{d_Y} (\mu_{a_{j,l}}^2 + \sigma_{a_{j,l}}^2 - \log(\sigma_{a_{j,l}}^2) - 1) \right] \quad (27) \end{aligned}$$

Hence, for any $j = 1, \dots, N$ and $l = 1, \dots, d_X$:

$$\begin{aligned} |\mu_{b_{j,l}}| &\leq \|\mu\|_2 \leq \sqrt{2\text{KL}(q_{\theta}^N | q_{\theta_0}^N)}, \\ \sigma_{b_{j,l}} &\leq \|\sigma\|_2 \leq |\sigma_{b_{j,l}} + 1 - 1| \leq |\sigma_{b_{j,l}}^2 - \log(\sigma_{b_{j,l}}^2) - 1| + 1 \leq 2\text{KL}(q_{\theta}^N | q_{\theta_0}^N) + 1, \end{aligned} \quad (28)$$

and

$$\mathbb{E}[|b_{j,l}|] \leq \sqrt{\frac{2}{\pi}}(2\text{KL}(q_{\theta}^N | q_{\theta_0}^N) + 1) + \sqrt{2\text{KL}(q_{\theta}^N | q_{\theta_0}^N)} := D(\text{KL}(q_{\theta}^N | q_{\theta_0}^N)) \quad (29)$$

Where D is increasing. Hence, since \mathbf{X} is compact, there exists C_X such that $\|x\|_1 \leq C_X$ and:

$$|\mathbb{E}[\sigma(\langle b_j, x \rangle)]| \leq C_0 + LC_X D(\text{KL}(q_{\theta}^N | q_{\theta_0}^N)) := E(\text{KL}(q_{\theta}^N | q_{\theta_0}^N), \mathbf{X}), \quad (30)$$

Where E is increasing in its first variable. Finally, since

$$N^{-1} \sum_{j=1}^N \|\mu_{a_j}\|_2 \leq N^{-1} \|\mu_a\|_1 \leq N^{-1} \sqrt{Nd_Y} \|\mu_a\|_2 \leq N^{-\frac{1}{2}} \sqrt{d_Y} \sqrt{2\text{KL}(q_{\theta}^N | q_{\theta_0}^N)},$$

the first moment of the predictive distribution can be upper bounded as:

$$\|\mathbb{E}_{\bar{w} \sim q_{\theta}}[f_{\bar{w}}(x)]\| \leq \frac{E(\text{KL}(q_{\theta}^N | q_{\theta_0}^N), X) \sqrt{d_Y} \sqrt{2\text{KL}(q_{\theta}^N | q_{\theta_0}^N)}}{\sqrt{N}} := \frac{\phi(\text{KL}(q_{\theta}^N | q_{\theta_0}^N), \mathbf{X}, d_Y)}{\sqrt{N}},$$

where ϕ is increasing in its first variable. \square

Lemma 9. Assume the conditions of Proposition 1 hold. Then there exists a function ψ depending only on $\text{KL}(q_{\theta}^N | q_{\theta_0}^N)$, \mathbf{X} , and d_Y such that G , increasing in its first variable, such that:

$$\mathbb{E}_{\bar{w} \sim q_{\theta}^N}[\|f_{\bar{w}}(x)\|^2] \leq \frac{\psi(\text{KL}(q_{\theta}^N | q_{\theta_0}^N), \mathbf{X}, d_Y)}{N}.$$

Proof. For a posterior of the form (22), we can write the second moment of the predictive distribution as:

$$\mathbb{E}_{\bar{w} \sim q_{\theta}^N}[\|f_{\bar{w}}(x)\|^2] = \frac{1}{N^2} \sum_{j=1}^N \mathbb{E}[\sigma_j^2] \mathbb{E}[\|a_j\|^2] + \frac{2}{N^2} \sum_{j=1}^N \sum_{k < j}^N \mathbb{E}[\sigma_j] \mathbb{E}[\sigma_k] \mathbb{E}[\langle a_j, a_k \rangle]. \quad (31)$$

We start with the second term on the right hand side of (31). Using $\mathbb{E}[\langle a_j, a_k \rangle] = \langle \mu_{a_j}, \mu_{a_k} \rangle \leq 1/2(\|\mu_{a_j}\|^2 + \|\mu_{a_k}\|^2)$, along with (28) and (30), we have

$$\frac{1}{N^2} \sum_{j=1}^N \sum_{k=1}^N \mathbb{E}[\sigma_j] \mathbb{E}[\sigma_k] \langle \mu_{a_j}, \mu_{a_k} \rangle \leq \frac{E^2(\text{KL}(q_{\theta}^N | q_{\theta_0}^N)) 2\text{KL}(q_{\theta}^N | q_{\theta_0}^N)}{N^2}.$$

We now turn to the first term on the right hand side of (31). We first have for any $j = 1, \dots, N$, using (27) that:

$$\mathbb{E}[\|a_j\|^2] = \sum_{l=1}^{d_Y} \mathbb{E}[a_{j,l}^2] = \sum_{l=1}^{d_Y} (\sigma_{a_{j,l}}^2 + \mu_{a_{j,l}}^2) \leq 2\text{KL}(q_{\theta}^N | q_{\theta_0}^N) + d_Y(2\text{KL}(q_{\theta}^N | q_{\theta_0}^N) + 1)^2 := F(\text{KL}(q_{\theta}^N | q_{\theta_0}^N)).$$

Then, using that σ is L -Lipschitz, Cauchy-Schwartz inequality and that since \mathbf{X} is compact there exists c_X such that $\|x\| \leq c_X$, we have:

$$\mathbb{E}[\sigma_j^2] \leq \mathbb{E}[(C_0 + L|\langle b_j, x \rangle|)^2] = C_0^2 + 2C_0 c_X L \mathbb{E}[|\langle b_j, x \rangle|] + L^2 c_X^2 \mathbb{E}[\|b_j\|^2],$$

where, using (27) and (29),

$$\begin{aligned} \mathbb{E}[\|b_j\|] &\leq \sum_{l=1}^{d_X} \mathbb{E}[|b_{j,l}|] \leq d_X D(\text{KL}(q_{\theta}^N | q_{\theta_0}^N)), \\ \mathbb{E}[\|b_j\|^2] &= \sum_{l=1}^{d_X} \mathbb{E}[b_{j,l}^2] = \sum_{l=1}^{d_X} (\sigma_{b_{j,l}}^2 + \mu_{b_{j,l}}^2) \leq d_X(2\text{KL}(q_{\theta}^N | q_{\theta_0}^N) + 1)^2 + 2\text{KL}(q_{\theta}^N | q_{\theta_0}^N). \end{aligned}$$

Hence,

$$\mathbb{E}[\sigma_j^2] \leq C_0^2 + 2C_0 c_X L d_X D(\text{KL}(q_{\theta}^N | q_{\theta_0}^N)) + L^2 c_X^2 2\text{KL}(q_{\theta}^N | q_{\theta_0}^N) := G(\text{KL}(q_{\theta^*}^N, q_{\theta_0}^N)),$$

with R increasing. Hence, the first term on the right hand side of (31) can be bounded as:

$$\frac{1}{N^2} \sum_{j=1}^N \mathbb{E}[\sigma_j^2] \mathbb{E}[\|a_j\|^2] \leq \frac{G(\text{KL}(q_{\theta^*}^N, q_{\theta_0}^N)) F(\text{KL}(q_{\theta^*}^N, q_{\theta_0}^N))}{N}.$$

Finally, we obtain the desired result with:

$$\psi(\text{KL}(q_{\theta^*}^N, q_{\theta_0}^N)) := G(\text{KL}(q_{\theta^*}^N, q_{\theta_0}^N)) F(\text{KL}(q_{\theta^*}^N, q_{\theta_0}^N)) + E^2(\text{KL}(q_{\theta^*}^N, q_{\theta_0}^N)) \sqrt{2\text{KL}(q_{\theta^*}^N, q_{\theta_0}^N)}.$$

□

Lemma 10. Let l be the cross-entropy loss, and $q_{\theta}^N \in \mathcal{F}_{\Theta}$ where \mathcal{F}_{Θ} is a family of Gaussians with diagonal covariance matrices, i.e. for any $\theta \in \Theta$, $\theta = (\mu, \sigma) \in \mathbb{R}^{N d_X} \times \mathbb{R}^{N d_Y}$. Assume that each coordinate of θ is bounded by a constant (independent of N) and that $\lim_{N \rightarrow \infty} \|\mathbb{E}_{\bar{w} \sim q_{\theta}}[f_{\bar{w}}(x)]\| = 0$ for any $x \in \mathcal{X}$. Then,

$$\lim_{N \rightarrow \infty} \mathcal{L}(q_{\theta}^N) = p(\log(d_Y) + \log(Z)).$$

Proof. For any $i = 1, \dots, p$, denote

$$\begin{aligned} l_{y_i} : \quad \mathbb{R}^{d_Y} &\longrightarrow \mathbb{R} \\ (z_1, \dots, z_{d_Y}) &\longmapsto -\log \left(\frac{e^{z_{y_i}}}{\sum_{j=1}^{d_Y} e^{z_j}} \right), \end{aligned}$$

so that $\forall z = (z_1, \dots, z_{d_Y}) \in \mathbb{R}^{d_Y}$,

$$|l_{y_i}(z)| = \left| -\log(\exp(z_{y_i}) + \log \left(\sum_{k=1}^{d_Y} \exp(z_k) \right)) \right|. \quad (32)$$

By the definition of \mathcal{L} and plugging $-\log(d_Y) - \log(Z)$ in (32), we have:

$$|\mathcal{L}(q_{\theta}^N) - p(\log(d_Y) + \log(Z))| \leq \sum_{i=1}^p |\mathbb{E}_{\bar{w} \sim q_{\theta}^N}[f_{\bar{w}}(x, y_i)]| + |\mathbb{E}_{\bar{w} \sim q_{\theta}^N}[\log \frac{1}{d_Y} \sum_{k=1}^{d_Y} e^{f_{\bar{w}}(x, k)}]|,$$

where $f_{\bar{w}}(x, k)$ denotes the k -th coordinate of $f_{\bar{w}}(x) \in \mathbb{R}^{d_Y}$ for $l = 1, \dots, d_Y$. The first term on the right hand side of the previous inequality converges to 0 as N goes to infinity by assumption. Hence, we can focus on the second term. For any $k = 1, \dots, d_Y$, since σ is L -Lipschitz,

$$f_{\bar{w}}(x, k) = \frac{1}{N} \sum_{j=1}^N \sigma(\langle b_j, x \rangle) a_{j,k} \leq \frac{1}{N} \sum_{j=1}^N C_0 a_{j,k} + \frac{L}{N} \sum_{j=1}^N \sum_{l=1}^{d_X} |b_{j,l}| |x_l| a_{j,k}.$$

Using the previous inequality along with Jensen's inequality, we have

$$\left| \mathbb{E}_{\bar{w} \sim q_{\theta}^N} \left[\log \left(\frac{1}{d_Y} \sum_{k=1}^{d_Y} e^{\frac{L}{N} \sum_{j=1}^N \sum_{l=1}^{d_X} |b_{j,l}| |x_l| a_{j,k}} \right) \right] \right| \leq \left| \log \frac{1}{d_Y} \sum_{k=1}^{d_Y} \prod_{j=1}^N \prod_{l=1}^{d_X} \mathbb{E}_{\bar{w} \sim q_{\theta}^N} \left[e^{\frac{L |b_{j,l}| |x_l| a_{j,k}}{N}} \right] \right|.$$

Since the posterior is of the form (22) we have for any index (j, k, l) :

$$\begin{aligned} \mathbb{E}_{\bar{w} \sim q_{\theta}^N} \left[e^{L \frac{|b_{j,l}| |x_l| a_{j,k}}{N}} \right] &\leq \mathbb{E}_{\bar{w} \sim q_{\theta}^N} \left[e^{L \frac{|b_{j,l}| |x_l| |a_{j,k}|}{N}} \right] \\ &= \mathbb{E}_{u \sim \mathcal{N}(0,1); v \sim \mathcal{N}(0,1)} \left[e^{\frac{L |\sigma_{b_{j,l}} u + \mu_{b_{j,l}}| |x_l| |\sigma_{a_{j,k}} v + \mu_{a_{j,k}}|}{N}} \right] \\ &\leq \mathbb{E}_{u \sim \mathcal{N}(0,1); v \sim \mathcal{N}(0,1)} \left[e^{\frac{|C b + C| |x| |C a + C|}{N}} \right], \end{aligned}$$

for some constant $C > 0$ since by assumption each coordinate of the variational parameter is bounded. By the dominated convergence theorem, when N goes to infinity we have:

$$\mathbb{E}_{u \sim \mathcal{N}(0,1); v \sim \mathcal{N}(0,1)} \left[e^{\frac{L|\sigma_{b_{j,l}} u + \mu_{b_{j,l}}| |x|(\sigma_{a_{j,k}} v + \mu_{a_{j,k}})}{N}} \right] = 1 + o\left(\frac{1}{N}\right).$$

Hence,

$$\left| \mathbb{E}_{\bar{w} \sim q_{\theta}^N} \left[\log \frac{1}{d_Y} \sum_{k=1}^{d_Y} e^{\frac{L}{N} \sum_{j=1}^N \sum_{l=1}^{d_X} |b_{j,l}| |x_l| a_{j,k}} \right] \right| \leq N d_X \log \left(1 + o\left(\frac{1}{N}\right) \right)$$

Similarly, we can prove that:

$$\lim_{N \rightarrow \infty} \left| \mathbb{E}_{\bar{w} \sim q_{\theta}^N} \left[\log \frac{1}{d_Y} \sum_{k=1}^{d_Y} e^{\frac{\sigma(0)}{N} \sum_{j=1}^N a_{j,k}} \right] \right| = 0$$

Finally, we have:

$$\lim_{N \rightarrow \infty} |\mathcal{L}(q_{\theta}^N) - p(\log(d_Y) + \log(Z))| \leq \lim_{N \rightarrow \infty} \left| N d_X \log \left(1 + o\left(\frac{1}{N}\right) \right) \right| = 0.$$

□

C Additional Experiments

C.1 Balanced ELBO with cooling

We first support with a very simple experiment the theoretical results of Section 3 and the relevance of the form of the parameter $\eta_N = \tau p/N$ we find. This experiment does not require training, since the goal here is to illustrate how introducing this parameter allows to balance the contributions of the two terms in the decomposition of ELBO_{η}^N in (6). We choose the architecture of a one hidden layer neural network with ReLU activation functions, to which we will refer to as *Linear BNN*. We consider a regression task on the Boston dataset and a classification task on MNIST. We choose a zero-mean Gaussian prior with variance $1/5$ for each neuron. Also, we initialize the variational parameters $\theta = (\mu, \sigma)$ where μ is close to zero and $\sigma = 10^{-3}$. Figure 3 and 4 illustrate the ratio between the likelihood and KL terms in ELBO_{η}^N when the number of weights grows, for $\eta_N = 1$ (no cooling), $\eta_N = \tau p/N$ and different values of the hyperparameter τ , on the MNIST and BOSTON datasets respectively. They confirm that when the number of data points p is fixed and ELBO_{η}^N is not rescaled, one of the two terms become dominant contrary to the case where we set $\eta_N = \tau p/N$.

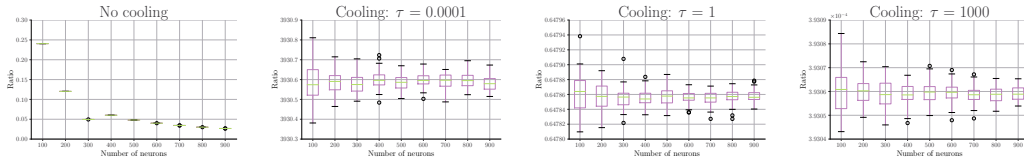


Figure 3: Ratio of the two ELBO_{η}^N terms, for a Linear BNN (non trained) on MNIST.

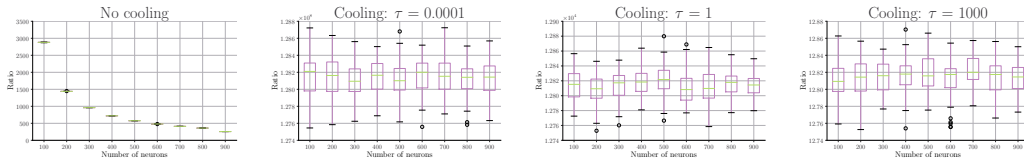


Figure 4: Ratio of the two ELBO_{η}^N terms, for a Linear BNN (non trained) on BOSTON.

C.2 ECE definition

For any input x , define $\text{conf}(x) = \max_{c \in \{1, \dots, n_l\}} \Psi_c(f_{\bar{w}}(x))$, i.e., the maximal predicted probability of the network. This quantity can be viewed as a prediction confidence for the input x . ECE discretizes the interval $[0, 1]$ into a given number of bins B and groups predictions based on the confidence score: $S_b = \{i \in \{1, \dots, p\}, \text{conf}(x_i) \in [b/B, (1+b)/B]\}$. The calibration error is the difference between the fraction of predictions in the bin that are correct (accuracy) and the mean of the probabilities in the bin (confidence).

$$\text{ECE} = \sum_{b=1}^B \frac{|S_b|}{p} |\text{acc}(S_b) - \text{conf}(S_b)|,$$

where p is the total number of data points, and $|S_b|$, $\text{acc}(S_b)$ and $\text{conf}(S_b)$ are the number of predictions, the accuracy and confidence of bin S_b respectively.

C.3 Cooling effect on the distribution of the variational parameters

Figure 5 illustrates the distribution of the variational parameters after training a linear BNN (i.e., single hidden layer with ReLU) on MNIST. For a large τ , the distribution of the variational parameters is close to the prior (a centered Gaussian with standard deviation 0.2). For a small τ , we can see that the network has learnt values of σ that are very different from the prior (e.g., close to zero). Intermediate values of τ interpolate between the two previous regimes

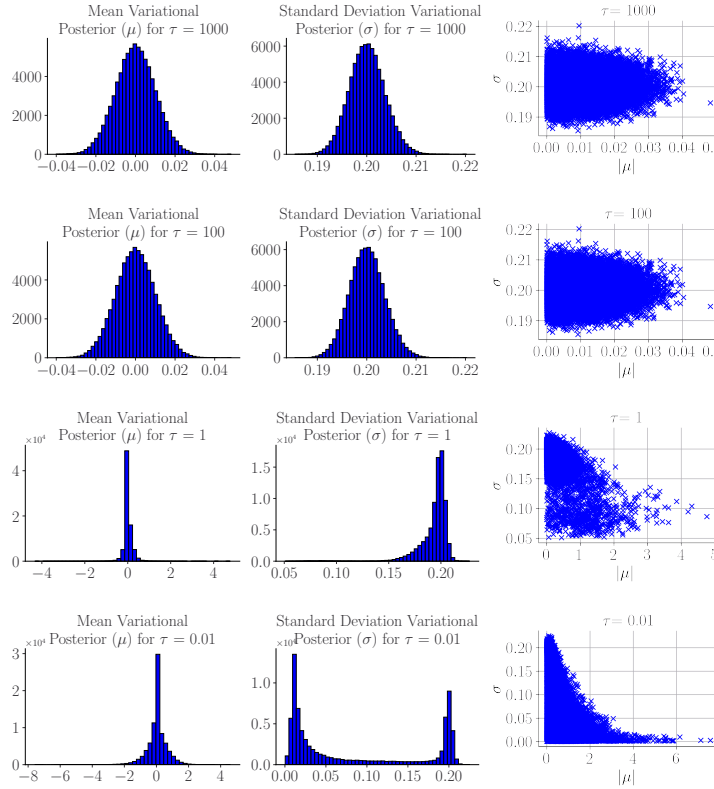


Figure 5: Histograms of the variational parameters $\theta = (\mu, \sigma)$ for a Linear BNN trained on MNIST. From left to right: histogram of variational means, standard deviations, and standard deviation as a function of the norm of the mean.

C.4 OOD detection

We also compare the performance on out-of-distribution of a Resnet20 trained on CIFAR-10 with Bayes by Backprop. We compute the the histogram of predictive entropies for 5000 in-distribution

samples and out-of-distribution samples. Recall that the negative entropy is defined for a vector of class probabilities $[p(y = c|x, \mathcal{D})]_{c \in \{1, \dots, n_l\}}$ as $-\sum_{c=1}^{n_l} p(y = c|x, \mathcal{D}) \log(p(y = c|x, \mathcal{D}))$. The first ones correspond to samples from the test set of CIFAR-10; while the out-of-distribution samples are chosen from another image dataset, namely SVHN [Netzer et al. \(2011\)](#). Our results are to be found in Figure 6 and illustrate again the importance of the parameter τ . When τ is very small, the model is highly confident for in-distribution samples, and has diffuse predictive entropies for out-distribution samples. As τ increases, the model starts to be less confident, resulting in higher entropies on both in-distribution and out-distribution samples, especially for the out-distribution samples. Finally if τ is too large, as the model sticks to the prior distribution, it is not confident neither on the in-distribution nor out-distribution, resulting on a spiky distribution of predictive entropies at high values.

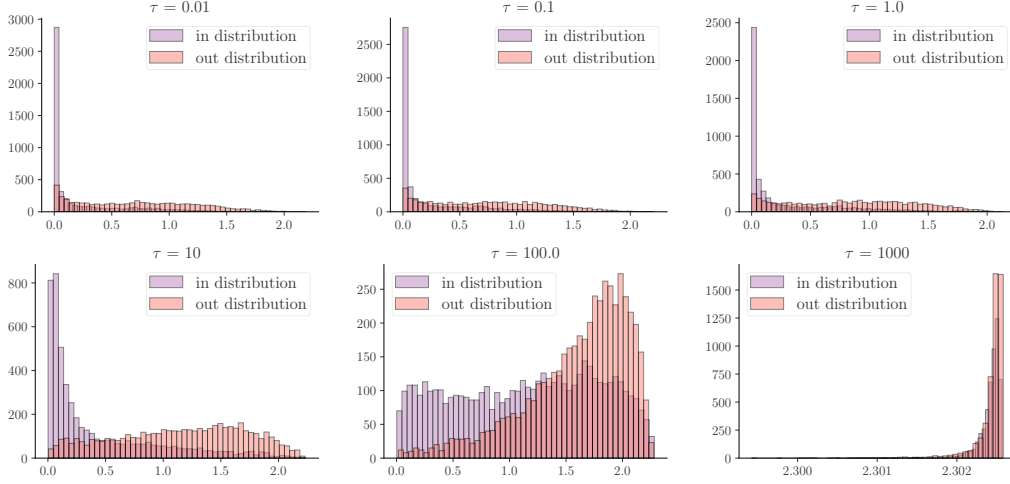


Figure 6: Histogram of the predictive entropies for a Resnet20 trained on CIFAR-10, on 5000 in-distribution (from the test set of CIFAR-10 dataset) and out-of-distribution (from SVHN dataset) samples

D Bayes by Backprop

Several methods have been proposed to optimize ELBO^N . A first and straightforward approach is to apply stochastic gradient descent (SGD), using samples from q_{θ_c} where θ_c is the current point, to obtain stochastic estimates for $\nabla_{\theta} \text{ELBO}^N$. However, the resulting estimation of the gradient suffers from high variance. Alternative algorithms have been proposed to mitigate this effect, such as Probabilistic Backpropagation [Hernández-Lobato and Adams \(2015\)](#) or Bayes by Backprop [Blundell et al. \(2015\)](#). Given a fixed distribution $\bar{\gamma}$ and a parameterized function $g(\theta, \cdot)$, the network parameter \bar{w} is obtained as $\bar{w} = g(\theta, z)$, where z is sampled from $\bar{\gamma}$, e.g., from a standard normal distribution. While a new z is sampled at each iteration, its distribution is constant, unlike that of the network parameters \bar{w} . As soon as $g(\theta, \cdot)$ is invertible and $\gamma, q(\cdot|\theta)$ are non-degenerated probability distributions, we have $q(\bar{w}|\theta)d\bar{w} = \bar{\gamma}(z)dz$ (see [Jospin et al. \(2020, Appendix A\)](#)), and for any differentiable function f :

$$\frac{\partial}{\partial \theta} \mathbb{E}_{\bar{w} \sim q(\cdot|\theta)} [f(\bar{w}, \theta)] = \mathbb{E}_{z \sim \bar{\gamma}} \left[\frac{\partial f(\bar{w}, \theta)}{\partial \theta} + \frac{\partial \bar{w}}{\partial \theta} \frac{\partial f(\bar{w}, \theta)}{\partial \bar{w}} \right].$$

Bayes by Backprop uses the previous equality to estimate the gradient of F , because $F = \mathbb{E}_{\bar{w} \sim q(\cdot|\theta)} [f(\bar{w}, \theta)]$ with $f(\bar{w}, \theta) = \log q(\bar{w}|\theta) - \log P_0(\bar{w}) - \log P(\mathcal{D}|\bar{w})$. More specifically, it performs a stochastic gradient descent for F using a new sample z at each time step to estimate the gradient of F as the parameter θ is updated. When the step size in this algorithm goes to zero, the Bayes by Backprop dynamics corresponds to a Wasserstein gradient flow of a particular functional defined on the space of probability distributions over θ , which we introduce in the next section.

Algorithm 1 Bayes by Backprop

Input: step-size $\delta > 0$, number of iterations m_{iter} , number of samples $M_{samples}$.

for each m_{iter} iterations **do**

for each $m = 1, \dots, M_{samples}$ **do**

 1. Sample $\mathbf{z} \sim \gamma^{\otimes N}$

 2. Let $\bar{w} = \boldsymbol{\mu} + \log(1 + \exp(\boldsymbol{\rho})) \odot \mathbf{z}$.

end for

 3. Compute

$$g(\bar{w}, \boldsymbol{\theta}) \approx \frac{1}{M_{samples}} \sum_{m=1}^{M_{batch}} \log q(\bar{w}_i | \boldsymbol{\theta}) - \log P_0(\bar{w}_i) P(\mathcal{D} | \bar{w}_i)$$

 5. Calculate the gradient with respect to the mean and standard deviation parameter ρ

$$\begin{aligned} \Delta_\mu &= \frac{\partial g(w, \theta)}{\partial w} + \frac{\partial g(w, \theta)}{\partial \mu} \\ \Delta_\rho &= \frac{\partial g(w, \theta)}{\partial w} \frac{\epsilon}{1 + \exp(\rho)} + \frac{\partial g(w, \theta)}{\partial \rho} \end{aligned}$$

 6. Update the variational parameters:

$$\begin{aligned} \mu &\leftarrow \mu - \delta \Delta_\mu \\ \rho &\leftarrow \rho - \delta \Delta_\rho \end{aligned}$$

end for

As in [Blundell et al. \(2015\)](#), we will use a variance reparameterization; $\sigma = \log(1 + \exp(\rho)) \in \mathbb{R}^+$ for $\rho \in \mathbb{R}$. Consequently, the variational parameter is given by $\boldsymbol{\theta} = (\theta_1, \dots, \theta_N) \in \mathbb{R}^{N \times 2d}$ with $\theta_j = (\mu_j, \rho_j) \in \mathbb{R}^{2d}$. We denote by $g : \mathbb{R}^{2d} \times \mathbb{R}^d \rightarrow \mathbb{R}$, $(\theta, z) \mapsto \mu + \log(1 + \exp(\rho)) \odot z$, where \odot denotes the entry-wise multiplication and γ denotes the standard normal distribution over \mathbb{R}^d . The Bayes-by-backprop algorithm in this setting is summarized in Algorithm 1.

This algorithm is well suited for minibatch optimisation, when the dataset \mathcal{D} is split into a partition of L subsets (minibatches) $\mathcal{D}_1, \dots, \mathcal{D}_L$. In this case [Graves \(2011\)](#) proposes to minimise a rescaled NELBO^N for each minibatch \mathcal{D}_l , $l = 1, \dots, L$ as

$$\text{NELBO}_l^N = \frac{1}{L} \text{KL}(q_{\boldsymbol{\theta}} | P_0) - \mathbb{E}_{\bar{w} \sim q_{\boldsymbol{\theta}}} [\log P(\mathcal{D}_l | \bar{w})].$$